Porous Materials

DOI: 10.1002/ange.201005176

Zeotype Organic–Inorganic Ionic Crystals: Facile Cation Exchange and Controllable Sorption Properties**

*Sayaka Uchida, Ryo Eguchi, and Noritaka Mizuno**

Storage and selective sorption of molecules by porous materials such as zeolites and metal–organic frameworks (MOFs) have been areas of intensive research because of their importance in industrial and environmental fields.[1] Recent studies have focused on rational design of porous materials by careful choice of precursors and starting materials.[1] For example, the pore sizes and volumes of Zn^{II} dicarboxylates are finely controlled by the lengths of the dicarboxylate ligands.[1j] On the other hand, ion exchange is a facile method to control the pore structures and sorption properties of porous materials.[2–7] Pore sizes and guest affinities of zeolites can be controlled by cation exchange. For example, K^+ resides in the pores of K-LTA zeolite, and the effective pore diameter is 3 Å. The effective pore size is increased to 4 Å by exchange of K^+ with the smaller Na^+.[2] The amounts of methane and water adsorbed by alkaline earth metal ion-exchanged and alkali metal ion-exchanged FAU zeolites increase with increasing ionic potential Z/r (Z and r are the charge and radius of the ion, respectively) of the countercations.[3,4] The control of pore structures and sorption properties of MOFs by ion exchange is still rare compared with zeolites. For example, the pore volumes of A^I indium tetracarboxylates,[5] and the H_2 sorption properties of M^{II} benzene tris-tetrazolates and A^I indium imidazole dicarboxylates[6] are largely controlled by the kind of cations (A^I: alkali metal ions, M^{II}: divalent transition metal cations). Ni^{2+}–1,2-bis(4-pyridyl)ethane shows anion-exchange properties, and exchange of $N(CN)_2^-$ with N_3^- leads to modification of the pore structure and the increase in the amount of adsorbed CO_2.[7]

Polyoxometalates are nanosized metal oxide multivalent anions and can form nanostructured ionic crystals in combination with appropriate cations.[8] Some ionic crystals have channels in the crystal lattice and can sorb guest molecules, and the sorption properties are finely tuned by the choice of starting materials.[8b,c,e,g–j] However, to the best of our knowledge, control of sorption properties by cation exchange has never been reported for polyoxometalate-based ionic crystals, probably because of the strong Coulomb interactions between the multivalent polyoxometalates and countercations. Here we report zeotype organic–inorganic ionic crystal $K_2[Cr_3O(OOCH)_6(mepy)_3]_2[\alpha\text{-}SiW_{12}O_{40}]\cdot 2H_2O\cdot CH_3OH$ (**1-K$^+$**, mepy = 4-methylpyridine) with one-dimensional channels occupied by K^+. The guest-free phase **2-K$^+$** sorbs water and methanol, while exclusion of larger molecules such as *n*-propanol, dichloromethane, and ethylene reveals size-selective sorption. More interestingly, the potassium ions in **1-K$^+$** can be exchanged with other alkali metal ions in water at room temperature without structure change, and the guest sorption properties of the guest-free phases **2-A$^+$** (A = Na, K, Rb, and Cs) largely depend on the alkali metal ion.

The structure of **1-K$^+$** is shown in Figure 1. The distances between adjacent mepy rings of about 3.5 and 4.0 Å are

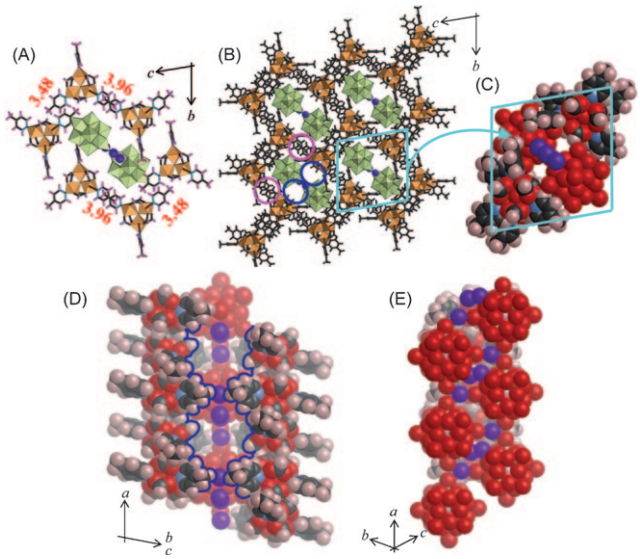

Figure 1. Crystal structure of **1-K$^+$**. A) Local structure showing the π–π interactions, B) arrangements of the constituent ions, C) narrowest opening of the channel, D) and E) cross sections of the channels from different views. Green and orange polyhedra in A) and B) correspond to $[WO_6]$ and $[CrO_5N]$ units, respectively. The figures in A) are distances between the mepy rings. Blue, pink, and black sticks in A) are C–N, C–H, and C–C bonds, respectively, and all of these bonds are shown in black in B). Purple spheres are potassium ions. Dark blue and pink ovals in B) are channels and spaces surrounded by the mepy ligands, respectively. Red, black, pink, and blue spheres in the space-filling models of C)–E) are oxygen, carbon, hydrogen, and nitrogen atoms, respectively. The dark blue lines in D) correspond to the channel walls.

[*] Dr. S. Uchida, R. Eguchi, Prof. Dr. N. Mizuno
Department of Applied Chemistry, School of Engineering
The University of Tokyo, 7-3-1 Hongo, Bunkyo-ku, Tokyo (Japan)
Fax: (+81) 3-5841-7220
E-mail: tmizuno@mail.ecc.u-tokyo.ac.jp

[**] This work was supported by the Core Research for Evolutional Science and Technology (CREST) program of the Japan Science and Technology Agency (JST), the Global COE Program (Chemistry Innovation through Cooperation of Science and Engineering), the Development in a New Interdisciplinary Field Based on Nanotechnology and Materials Science Programs, and Grant-in-Aid for Scientific Research from the Ministry of Education, Culture, Science, Sports, and Technology of Japan.

Supporting information for this article is available on the WWW under http://dx.doi.org/10.1002/anie.201005176.

indicative of π–π interactions (Figure 1 A), and polyoxometalates and K^+ are surrounded by the macrocations (Figure 1 B). Compound **1-K**$^+$ has one-dimensional channels along the *a* axis. The channel walls are composed of polyoxometalate anions and macrocations, and K^+ is located in the channels. Figure 1 C shows the narrowest opening of the channel, and Figure 1 D and E show the cross section of the channel from different views. The potassium ions are located in the vicinity of the polyoxometalate anions (K–O ca. 3.0 Å). The channels are winding and the narrowest cross section area of the opening is about 25 Å^2. The volume of the channel, shown by the dark blue ovals in Figure 1 B, was calculated to be 159 Å^3 per formula unit (2.17×10^{-2} cm^3 g^{-1}) with the PLATON program.[9] Besides the channel, two kinds of spaces are present, indicated by the pink ovals in Figure 1 B. These spaces are surrounded by the mepy ligands and are accessible from the channels. The volumes of both of these spaces are 35–40 Å^3 per formula unit ($4.79–5.47\times10^{-3}$ cm^3 g^{-1}). Thus, the total void volume of **1-K**$^+$ is 234 Å^3 per formula unit (3.20×10^{-2} cm^3 g^{-1}).

Compound **1-K**$^+$ contained water and methanol as solvent molecules, which were desorbed by evacuation at 298–303 K for 3 h to give guest-free phase **2-K**$^+$. The powder XRD pattern of **1-K**$^+$ agreed well with that calculated from the single-crystal data (Figure S1A, Supporting Information). The powder XRD pattern of **2-K**$^+$ was slightly different from that of **1-K**$^+$, and its lattice parameters were calculated by Pawley refinement (Figure S1B, Supporting Information).[10] The changes in the lattice lengths and volume from **1-K**$^+$ to **2-K**$^+$ were −2.5–+0.5% and −3.5%, respectively. The sorption properties of **2-K**$^+$ were investigated by recoding sorption–desorption isotherms (298 K). As shown in Figure 2,

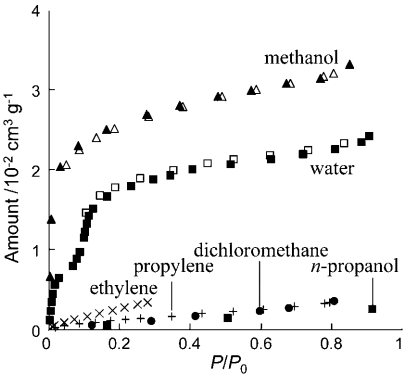

Figure 2. Sorption–desorption isotherms of **2-K**$^+$ for various compounds at 298 K. Full and empty symbols indicate sorption and desorption branches, respectively.

2-K$^+$ sorbed water (cross-sectional area: 10.5 Å^2) and methanol (17.9 Å^2).[11] The desorption plots overlapped with the sorption plots, and hysteresis was not observed. Larger ethylene (20.5 Å^2), propylene (25.7 Å^2), dichloromethane (24.4 Å^2), and *n*-propanol (27.1 Å^2) molecules were excluded. Thus, **2-K**$^+$ shows size-selective sorption properties.

Next, the exchange of K^+ in **1-K**$^+$ with other alkali metal ions (Na^+, Rb^+, and Cs^+) was attempted. The sorption properties of zeolites,[2–4] MOFs,[5–7] and layered compounds[12] can be finely controlled by cation exchange, because 1) the size of the channel opening can be controlled by that of the cation and/or 2) the cation can act as a site for guest sorption, and the host–guest interaction can be controlled by the ionic potential *Z*/*r* of the cation. The powder XRD patterns of **1-Na**$^+$, **1-Rb**$^+$, and **1-Cs**$^+$ (Figure S2, Supporting Information) are similar to that of **1-K**$^+$.[13] The narrowest cross section of the channel of **1-Cs**$^+$ is very similar to that of **1-K**$^+$, that is, the size of the channel opening is hardly changed by the exchanging K^+ for the larger Cs^+ (Figure S3, Supporting Information). Immersion of **1-Na**$^+$ and **1-Cs**$^+$ in an aqueous solution of KNO_3 at room temperature gave **1-K**$^+$, that is, cation exchange of the zeotype organic–inorganic ionic crystal occurs reversibly in water at room temperature without changes in the structure.

Water sorption isotherms of **2-A**$^+$ at 298 K (Figure 3 A) consist of two steps, and the sorbed amounts after the first step were about 2 mol mol^{-1} (ca. 1×10^{-2} cm^3 g^{-1}) for all

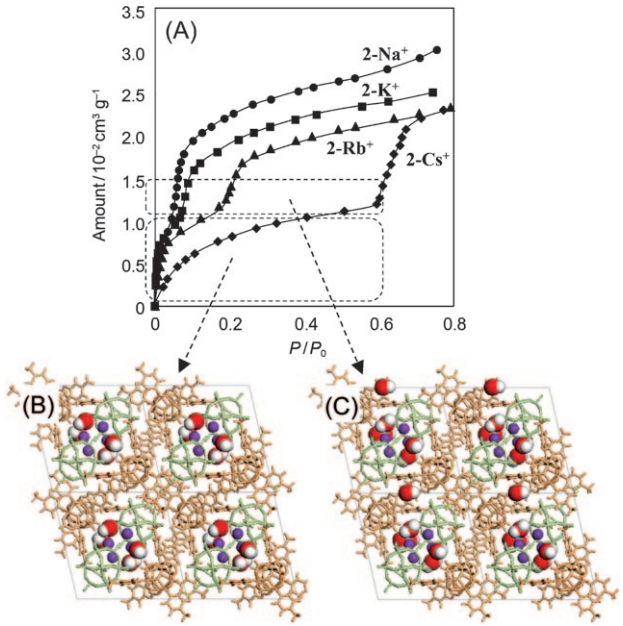

Figure 3. A) Water sorption isotherms of **2-A**$^+$ at 298 K. B) and C) Geometrical optimization of 2 mol mol^{-1} and 3 mol mol^{-1} of water molecules in **2-K**$^+$, respectively.

compounds. The desorption plots overlapped with the sorption plots and no hysteresis was observed (Figure S4, Supporting Information). The amounts of water sorbed under constant vapor pressure increased in the order **2-Cs**$^+$ < **2-Rb**$^+$ < **2-K**$^+$ < **2-Na**$^+$. The same order was observed for water sorption by alkali metal ion-exchanged FAU zeolites, and this order is explained by the ion–dipole interactions between host and guest, which increase with increasing ionic potential of the alkali metal ions.[4,14] The amount of methanol sorbed by **2-Cs**$^+$ (Figure S5, Supporting Information) was very small (ca. 5×10^{-3} cm^3 g^{-1} = 1 mol mol^{-1}) below $P/P_0<0.4$, and a gate pressure was observed around $P/P_0=0.4$. On the other hand, **2-K**$^+$ showed pronounced sorption even at very low

relative pressures (Figure 2). The change in the methanol sorption property can be explained by the increased ion–dipole interaction between host and guest because of the higher ionic potential of K^+.

This hypothesis was supported by geometrical optimization (Figure 3B and C) and the in situ IR spectrum (Figure S6, Supporting Information) of the water molecules sorbed in **2-K**$^+$. The first 2 mol mol^{-1} of water molecules sorbed are located in the vicinity of the potassium ions (K···O < 3.5 Å) (Figure 3B) and the remaining 1 mol mol^{-1} of sorbed water molecules are located either in the space left in the channels or in the space surrounded by the mepy ligands (Figure 3C).[16] The states of water molecules sorbed in **2-K**$^+$ can be characterized by in situ IR spectroscopy, since the ν(OH) bands shift to lower wavenumbers due to hydrogen bonding.[17] The in situ IR spectrum of the water molecules sorbed in **2-K**$^+$ at 298 K and $P/P_0 = 0.75$ showed a broad band in the range of 2700–3600 cm^{-1} (Figure S6, Supporting Information). The broad band was deconvoluted into three bands at 3470, 3300, and 3050 cm^{-1} with integrated intensity ratio of 2:1:1. According to the assignments of the water molecules sorbed in zeolites,[18] layered compounds,[19] and carbon nanotubes,[20] the bands at 3470, 3300, and 3050 cm^{-1} were respectively assigned to the ν(OH) bands of water molecules sorbed on the potassium ion, those in the channel, those within hydrogen-bonding distance of the oxygen atoms of the polyoxometalate anion and/or macrocation, and those in the space surrounded by the mepy ligands, which probably experience OH–π interaction.

To investigate the water sorption kinetics of **2-A**$^+$, the amounts of sorbed water as a function of time were measured. Figure 4 shows the experimental water sorption profiles of **2-A**$^+$ at water vapor pressures giving similar amounts of sorption at equilibrium ($M_e \approx 1.0 \times 10^{-2}$ cm^3 g^{-1}). The sorbed amounts increased and leveled off after about 1500, 800, 250, and 150 s for **2-Na**$^+$, **2-K**$^+$, **2-Rb**$^+$, and **2-Cs**$^+$, respectively. The experimental profiles were fitted with the Fickian diffusion model,[21] and the calculated profiles are shown along with the experimental profiles.[23] The diffusion coefficients increased in the order **2-Na**$^+$ (1.1×10^{-12}) < **2-K**$^+$ (3.3×10^{-12}) < **2-Rb**$^+$ (7.6×10^{-12}) < **2-Cs**$^+$ (1.5×10^{-11} cm^2 s^{-1}), and thus increases with decreasing ionic potential of the alkali metal ions, which suggests that water diffusion is controlled by the type of alkali metal ion. The same order was observed for water diffusion in small- to medium-pore alkali metal ion-exchanged zeolites such as LTA (pore diameter: 3–5 Å) and MFI (pore dimensions: (5.7–5.8) × (5.1–5.2) Å^2). This order is explained by the strong ion–dipole interactions between the alkali metal ions and water molecules resulting in clustering and immobilization of water molecules around the ions.[24] On the other hand, water diffusivities in large-pore alkali metal ion-exchanged zeolites such as FAU (pore diameter: 8–12 Å) and alkali metal ion-exchanged polymers such as Nafion increase with increasing ionic potential of the cation.[25] Since the channels of **2-A**$^+$ are one-dimensional and their openings are small and comparable to the size of a methanol molecule, strong ion–dipole interactions between the alkali metal ions and water molecules probably hinder diffusion of water in the channels.

In conclusion, zeotype organic–inorganic ionic crystal $K_2[Cr_3O(OOCH)_6(mepy)_3]_2[\alpha\text{-}SiW_{12}O_{40}]$ shows size-selective sorption and cation-exchange properties. The exchanged cations control the guest-sorption properties, and such facile cation exchange may be applicable to the production of novel sorbents for storage and selective sorption processes.

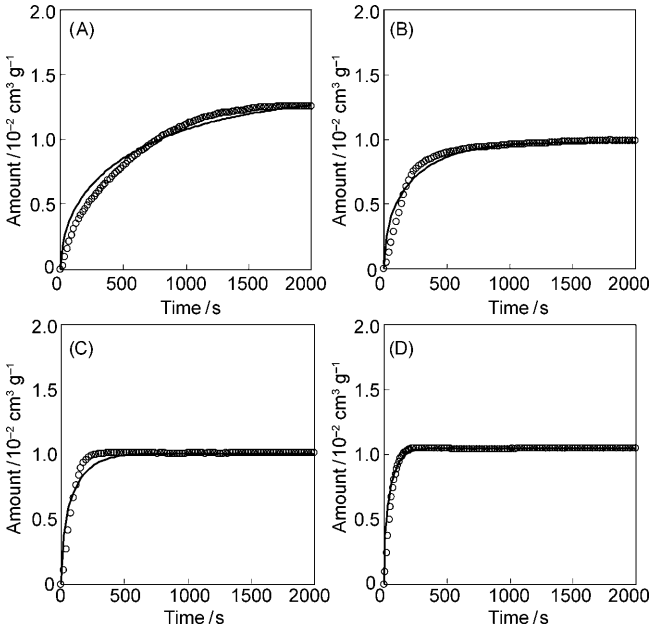

Figure 4. Amounts of water sorbed at 303 K as a function of time. A) **2-Na**$^+$ ($P/P_0 = 0.05$), B) **2-K**$^+$ ($P/P_0 = 0.13$), C) **2-Rb**$^+$ ($P/P_0 = 0.24$), and D) **2-Cs**$^+$ ($P/P_0 = 0.63$). The circles indicate experimental data, and black lines calculated data according to the Fickian diffusion model.

Experimental Section

Synthesis of $K_2[Cr_3O(OOCH)_6(mepy)_3]_2[\alpha\text{-}SiW_{12}O_{40}]\cdot 2H_2O\cdot CH_3OH$ (**1-K**$^+$): $H_4[\alpha\text{-}SiW_{12}O_{40}]\cdot n H_2O$[26] (0.75 g) and CH_3COOK (0.5 g) were dissolved in 160 mL of methanol (solution A). $[Cr_3O(OOCH)_6(mepy)_3](ClO_4)\cdot n H_2O$[27] (0.5 g) was dissolved in 120 mL of 1,2-dichloroethane, and then CH_3COOK (0.5 g) dissolved in the minimum amount of methanol was added. This solution was filtered to remove $KClO_4$ (solution B). Solution A was added to solution B with vigorous stirring, and the resulting solution was kept at 298 K for 24 h. Brown crystals of **1-K**$^+$ were isolated in 50% yield. FTIR: 1641 (br), 1375 (m), 973 (m, ν_{asym}(W=O)), 923 (br, ν_{asym}(Si–O)), 888 (w, ν_{asym}(W-O$_c$-W)), 801 (br, ν_{asym}(W-O$_e$-W)), 641 cm^{-1} (m, ν_{asym}(Cr_3O)). Elemental analysis calcd for **1-K**$^+$: C 13.19, H 1.40, N 1.88, Cr 6.99, K 1.75, Si 0.63, W 49.43; found: C 13.20, H 1.56, N 1.87, Cr 7.09, K 1.74, Si 0.63, W 49.17.

Exchange of K^+ in **1-K**$^+$ with Na^+, Rb^+, or Cs^+: **1-K**$^+$ (0.25 g) was added to an aqueous solution of $NaNO_3$, $RbNO_3$, or $CsNO_3$ (1M, 10 mL), and the solution was stirred at 298 K for 24 h followed by filtration and washing of the solid. This procedure was repeated. Cation exchange proceeded at lower concentrations (e.g., 0.3M) and with other salts (e.g., chlorides). The present conditions (1M of nitrates) were chosen because higher concentrations (i.e., smaller solution volumes) shorten the filtration time and the solubilities of alkali metal nitrates in water are high. The chemical formulas of **1-Na**$^+$, **1-Rb**$^+$, and **1-Cs**$^+$ (Table 1) were determined by inductively coupled plasma atomic emission spectroscopy and atomic absorption spectroscopy. The elemental analyses of the filtrates showed that leaching of polyoxometalate did not occur. The leached amount of

Table 1: Chemical formulas of **1-Na**$^+$, **1-K**$^+$, **1-Rb**$^+$, and **1-Cs**$^+$.

1-Na$^+$	$K_{0.1}Na_{1.9}[Cr_3O(OOCH)_6(mepy)_3]_2[\alpha\text{-}SiW_{12}O_{40}]\cdot 4H_2O$
1-K$^+$	$K_{2.0}[Cr_3O(OOCH)_6(mepy)_3]_2[\alpha\text{-}SiW_{12}O_{40}]\cdot 2H_2O\cdot CH_3OH$
1-Rb$^+$	$K_{0.1}Rb_{1.9}[Cr_3O(OOCH)_6(mepy)_3]_2[\alpha\text{-}SiW_{12}O_{40}]\cdot 4H_2O$
1-Cs$^+$	$K_{0.1}Cs_{1.9}[Cr_3O(OOCH)_6(mepy)_3]_2[\alpha\text{-}SiW_{12}O_{40}]\cdot 4H_2O$

macrocation of about 1% was probably due to exchange of $[Cr_3O(OOCH)_6(mepy)_3]^+$ with alkali metal ions. Notably, synthesis of **1-Na**$^+$, **1-Rb**$^+$, and **1-Cs**$^+$ by substitution of CH_3COOK with the corresponding acetates in the synthetic procedure of **1-K**$^+$ was unsuccessful.

Guest-free phases **2-A**$^+$ were prepared by evacuation of **1-A**$^+$ or exposure of **1-A**$^+$ to a dry N_2 or He gas at 298–303 K for 3 h. The IR spectra of **2-A**$^+$ showed characteristic bands of the macrocations and polyoxometalate anions, indicating that the molecular structures of the constituent ions were retained on loss of the solvent molecules.

Single-crystal X-ray diffraction: Diffraction measurements and structure analyses were performed on a Rigaku Saturn diffractometer with graphite-monochromated $Mo_{K\alpha}$ radiation ($\lambda = 0.71069$ Å) and a CCD 2D detector and Crystal structure crystallographic software package (Rigaku/MSC), respectively. A single crystal of **1-K**$^+$ was immersed in Araldite paste and mounted on a glass capillary, and the diffraction data were collected at 153 K. The structure was solved by direct methods, expanded by Fourier techniques, and refined by full-matrix least-squares calculations on F^2. Three crystallographically independent potassium ions were located with occupancies of 0.76, 0.71, and 0.53. The solvent molecules and hydrogen atoms were not included in the calculations. The tungsten and chromium atoms were refined anisotropically, while other atoms were refined isotropically. The potential solvent area (i.e., channel volume) of **1-K**$^+$ was calculated with PLATON by including the geometrically located hydrogen atoms.[9] CCDC 785157 contains the supplementary crystallographic data for this paper. These data can be obtained free of charge from The Cambridge Crystallographic Data Centre via www.ccdc.cam.ac.uk/data_request/cif. Crystal data for **1-K**$^+$: Triclinic $P\bar{1}$, $a = 13.523(4)$, $b = 20.353(4)$, $c = 20.355(5)$ Å, $\alpha = 74.936(2)$, $\beta = 71.939(8)$, $\gamma = 71.974(8)°$, $V = 4980.91(2)$ Å^3, $Z = 2$, $\rho_{calcd} = 2.895$ g cm^{-3}, crystal size $0.10 \times 0.10 \times 0.02$ mm^3, $T = 153.1$ K, $\mu(Mo_{K\alpha}) = 14.630$ cm^{-1}, 26388 reflections collected, 672 parameters, $R_1[I > 2\sigma(I)] = 0.1071$, $wR_2 = 0.3320$, GOF = 1.541. Structure analysis with a Laue class of higher symmetry failed.

Powder X-ray diffraction: Powder X-ray diffraction (XRD) patterns were measured with an XRD-DSCII (Rigaku Corporation) and $Cu_{K\alpha}$ radiation ($\lambda = 1.54056$ Å, 50 kV, 300 mA) at 303 K. The diffraction data were collected in the range of $2\theta = 4$–$38°$ at 0.01° points and 5 s/step. The measurements for **1-A**$^+$ and **2-A**$^+$ were carried out under ambient conditions and under a dry N_2 flow, respectively. The crystallographic parameters were calculated by using Materials Studio Softwares (Accelrys Inc.) by unit-cell indexing and space-group determination with X-cell followed by peak profile fitting by Pawley refinement.[10,28]

Received: August 18, 2010
Published online: November 17, 2010

Keywords: ion exchange · microporous materials · organic–inorganic hybrid composites · polyoxometalates · shape-selective sorption

[1] a) K. Oisaki, Q. Li, H. Furukawa, A. U. Czaja, O. M. Yaghi, *J. Am. Chem. Soc.* **2010**, *132*, 9262; b) H. Deng, C. J. Doonan, H. Furukawa, R. B. Ferreira, J. Towne, C. B. Knobler, B. Wang, O. M. Yaghi, *Science* **2010**, *327*, 846; c) O. K. Farha, C. D. Malliakas, M. G. Kanatzidis, J. T. Hupp, *J. Am. Chem. Soc.* **2010**, *132*, 950; d) J. Jiang, J. L. Jorda, M. J. Diaz-Cabanas, J. Yu, A. Corma, *Angew. Chem.* **2010**, *122*, 5106; *Angew. Chem. Int. Ed.* **2010**, *49*, 4986; e) S. Horike, S. Shimomura, S. Kitagawa, *Nat. Chem.* **2009**, *1*, 695; f) T. Yamada, H. Kitagawa, *J. Am. Chem. Soc.* **2009**, *131*, 6312; g) L. Alaerts, C. E. A. Kirschhock, M. Maes, M. A. van der Veen, V. Finsy, A. Depla, J. A. Martens, G. V. Baron, P. A. Jacobs, J. F. M. Denayer, D. E. De Vos, *Angew. Chem.* **2007**, *119*, 4371; *Angew. Chem. Int. Ed.* **2007**, *46*, 4293; h) C. Serre, C. Mellot-Draznieks, S. Surblé, N. Audebrand, Y. Filinchuk, G. Férey, *Science* **2007**, *315*, 1828; i) A. J. Fletcher, K. M. Thomas, M. J. Rosseinsky, *J. Solid State Chem.* **2005**, *178*, 2491; j) M. Eddaoudi, J. Kim, N. Rosi, D. Vodak, J. Wachter, M. O'Keeffe, O. M. Yaghi, *Science* **2002**, *295*, 469; k) M. E. Davis, *Nature* **2002**, *417*, 813; l) S. M. Kuznicki, V. A. Bell, S. Nair, H. W. Hillhouse, R. M. Jacubinas, C. M. Braunbarth, B. H. Toby, M. Tsapatsis, *Nature* **2001**, *412*, 720; m) T. J. Barton, L. M. Bull, W. G. Klemperer, D. A. Loy, B. McEnaney, M. Misono, P. A. Monson, G. Pez, G. W. Scherer, J. C. Vartuli, O. M. Yaghi, *Chem. Mater.* **1999**, *11*, 2633.

[2] D. W. Breck, W. G. Eversole, R. M. Milton, T. B. Reed, T. L. Thomas, *J. Am. Chem. Soc.* **1956**, *78*, 5963.

[3] O. Talu, S. Y. Zhang, D. T. Hayhurst, *J. Phys. Chem.* **1993**, *97*, 12894.

[4] O. M. Dzhigit, A. V. Kiselev, K. N. Mikos, G. G. Muttik, T. A. Rahmanova, *Trans. Faraday Soc.* **1971**, *67*, 458.

[5] S. Yang, X. Lin, A. J. Blake, G. S. Walker, P. Hubberstey, N. R. Champness, M. Schröder, *Nat. Chem.* **2009**, *1*, 487.

[6] a) M. Dincă, J. R. Long, *J. Am. Chem. Soc.* **2007**, *129*, 11172; b) F. Nouar, J. Eckert, J. F. Eubank, P. Forster, M. Eddaoudi, *J. Am. Chem. Soc.* **2009**, *131*, 2864.

[7] T. K. Maji, R. Matsuda, S. Kitagawa, *Nat. Mater.* **2007**, *6*, 142.

[8] a) A. M. Todea, A. Merca, H. Bögge, T. Glaser, J. M. Pigga, M. L. K. Langston, T. Liu, R. Prozorov, M. Luban, C. Schröder, W. H. Casey, A. Müller, *Angew. Chem.* **2010**, *122*, 524; *Angew. Chem. Int. Ed.* **2010**, *49*, 514; b) S. Noro, R. Tsunashima, Y. Kamiya, K. Uemura, H. Kita, L. Cronin, T. Akutagawa, T. Nakamura, *Angew. Chem.* **2009**, *121*, 8859; *Angew. Chem. Int. Ed.* **2009**, *48*, 8703; c) H. Tagami, S. Uchida, N. Mizuno, *Angew. Chem.* **2009**, *121*, 6276; *Angew. Chem. Int. Ed.* **2009**, *48*, 6160; d) H. Tan, Y. Li, Z. Zhang, C. Qin, X. Wang, E. Wang, Z. Su, *J. Am. Chem. Soc.* **2007**, *129*, 10066; e) C. Streb, D. Long, L. Cronin, *Chem. Commun.* **2007**, 471; f) S. S. Mal, U. Kortz, *Angew. Chem.* **2005**, *117*, 3843; *Angew. Chem. Int. Ed.* **2005**, *44*, 3777; g) R. Kawamoto, S. Uchida, N. Mizuno, *J. Am. Chem. Soc.* **2005**, *127*, 10560; h) Y. Ishii, Y. Takenaka, K. Konishi, *Angew. Chem.* **2004**, *116*, 2756; *Angew. Chem. Int. Ed.* **2004**, *43*, 2702; i) M. V. Vasylyev, R. Neumann, *J. Am. Chem. Soc.* **2004**, *126*, 884; j) S. Uchida, M. Hashimoto, N. Mizuno, *Angew. Chem.* **2002**, *114*, 2938; *Angew. Chem. Int. Ed.* **2002**, *41*, 2814.

[9] A. L. Spek, PLATON, A Multipurpose Crystallographic Tool, Utrecht University, The Netherlands, **1980**.

[10] G. S. Pawley, *J. Appl. Crystallogr.* **1981**, *14*, 357.

[11] The surface area calculated from the N_2 adsorption isotherm of **2-K**$^+$ at 77 K was less than 2 m^2 g^{-1}, that is, N_2 molecules (cross-sectional area: 16.2 Å^2) cannot access the channels of **2-K**$^+$ at 77 K. On the other hand, the large amount of methanol sorbed at 298 K (Figure 2) shows that methanol molecules (cross-sectional area: 17.9 Å^2) easily diffuse through the channels of **2-K**$^+$ at 298 K. A similar significant decrease in the amount of ethane sorbed from 298 to 195 K was observed for $K_2[Cr_3O(OOCH)_6(C_5H_5N)_3]_2[Cr_3O(OOCH)_6(C_5H_5N)(CH_3OH)_2]_{0.5}[\alpha\text{-}SiW_{12}O_{40}]$. These discrepancies are probably due to the slow diffusion of guest molecules and/or a small contraction of the unit cell at the low temperatures.

[12] R. W. Mooney, A. G. Keenan, L. A. Wood, *J. Am. Chem. Soc.* **1952**, *74*, 1371.

[13] The powder XRD pattern of **1-Cs**$^+$ was slightly different from those of **1-Na**$^+$, **1-K**$^+$, and **1-Rb**$^+$. The calculated lattice constants of **1-Cs**$^+$ were $a = 13.390$, $b = 20.266$, $c = 20.451$ Å, $\alpha = 75.544$, $\beta = 72.464$, $\gamma = 72.848°$, $V = 4977.0$ Å^3, and almost the same as those of **1-K**$^+$.

[14] Ionic radii of the alkali metal ions[15] are 1.16, 1.52, 1.66, and 1.81 Å for Na^+, K^+, Rb^+, and Cs^+, respectively, and thus the ionic potentials Z/r increase in the order $Cs^+ < Rb^+ < K^+ < Na^+$.

[15] R. D. Shannon, *Acta Crystallogr. Sect. A* **1976**, *32*, 751.

[16] Geometrical optimization of water sorbed in **2-Cs**$^+$ also showed that the first 2 mol mol^{-1} of water molecules sorbed are located in the vicinity of the cesium ions, and the next 1 mol mol^{-1} either in the space left in the channels or in the space surrounded by the mepy ligands.

[17] G. C. Pimentel, A. L. McClellan, *The Hydrogen Bond*, W. H. Freeman and Company, San Francisco–London, **1960**.

[18] a) I. A. Beta, H. Böhlig, B. Hunger, *Phys. Chem. Chem. Phys.* **2004**, *6*, 1975; b) J. W. Ward, *J. Phys. Chem.* **1968**, *72*, 4211.

[19] W. Xu, C. T. Johnson, P. Parker, S. F. Agnew, *Clays Clay Miner.* **2000**, *48*, 120.

[20] C. Feng, R. Q. Zhang, S. L. Dong, T. A. Niehaus, T. Frauenheim, *J. Phys. Chem. C* **2007**, *111*, 14131.

[21] Guest sorption into micropores is generally explained by the calculation with a Fickian diffusion equation for a system of uniform spherical particles[22]

$$\frac{\partial C}{\partial t} = D\left\{\frac{\partial^2 C}{\partial r^2} + \frac{2}{r}\left(\frac{\partial C}{\partial r}\right)\right\} \qquad \text{(i)},$$

where C, D, and r are the concentration, diffusion coefficient, and radial coordinate, respectively. The solution is given by

$$\frac{M_t}{M_e} = 1 - \frac{6}{\pi^2}\sum_{n=1}^{\infty}\left(\frac{1}{n^2}\right)\exp\left(\frac{-Dn^2\pi^2 t}{a^2}\right) \qquad \text{(ii)},$$

where M_t, M_e, and a are the uptake at time t, uptake at equilibrium, and particle radius, respectively.

[22] J. Crank, *The Mathematics of Diffusion*, Oxford University Press, London, **1956**.

[23] Discrepancies between the experimental profiles and those calculated with the Fickian diffusion equation increased in the order **2-Cs**$^+$ < **2-Rb**$^+$ < **2-K**$^+$ < **2-Na**$^+$, probably because binding of water molecules on the alkali metal ions becomes influential with increasing ionic potential of alkali metal ions.

[24] a) M. U. Ari, M. G. Ahunbay, M. Yurtsever, A. Erdem-Şenatalar, *J. Phys. Chem. B* **2009**, *113*, 8073; b) C. Corsaro, V. Crupi, D. Majolino, P. Migliardo, V. Venuti, U. Wanderlingh, T. Mizota, M. Telling, *Mol. Phys.* **2006**, *104*, 587; c) H. Paoli, A. Méthivier, H. Jobic, C. Krause, H. Pfeifer, F. Stallmach, J. Kärger, *Microporous Mesoporous Mater.* **2002**, *55*, 147.

[25] a) M. Legras, Y. Hirata, Q. T. Nguyen, D. Langevin, M. Métayer, *Desalination* **2002**, *147*, 351; b) C. Parravano, J. D. Baldeschwieler, M. Boudart, *Science* **1967**, *155*, 1535.

[26] J. C. Bailar, *Inorg. Synth.* **1939**, *1*, 132.

[27] M. K. Johnson, D. B. Powell, R. D. Cannon, *Spectrochim. Acta Part A* **1981**, *37*, 995.

[28] M. A. Neumann, *J. Appl. Crystallogr.* **2003**, *36*, 356.

